

# Fluctuating Flow Due to Unsteady Rotation of a Disk

P. Singh,\* V. Radhakrishnan,† and K. A. Narayan‡  
*Indian Institute of Technology at Kanpur, Kanpur, India*

The flow in a viscous fluid caused by the unsteady rotation of a porous disk is investigated. The governing equations are transformed into new coordinates with finite ranges by means of a transformation that maps an infinite interval into a finite one and are then solved by a finite-difference scheme. Computations have been carried out for short and long time ranges. The amplitude of oscillations of the tangential skin friction increases with the frequency parameter, whereas that of the radial skin friction decreases. However, the fluctuations in the angular velocity of the disk only slightly affect the surface heat transfer.

## Introduction

MANY current aerodynamic problems involve accelerated or decelerated rocket missiles, blades rotating in nonuniform airstreams, unsteady nozzle flow, oscillating wings, etc. In order to determine the friction drag and rate of heat transfer through the surface for such unsteady motions, the nature of the time-dependent oscillating flow of a fluid past a disk must be investigated. Attempts to obtain practical solutions, exact or approximate, to complete a set of governing equations resulting from the introduction of time into the analysis lead to great difficulties. Consequently, most investigators have studied the fluctuating flows with zero mean.<sup>2-5</sup> They considered the flow due to a disk, the angular velocity of which was taken as  $\Omega \cos \bar{\omega} \bar{t}$ . The study of fluctuating flows with nonvanishing mean was initiated by Lighthill,<sup>6</sup> who assumed the amplitude of the oscillations to be small and solved the problem by considering first-order perturbations to the basic steady flow. Lighthill's technique was extended to rotating flows by Purushothaman<sup>7</sup> and Sharma,<sup>8</sup> who obtained the flowfield when the disk rotates with angular velocity  $\Omega(1 + \epsilon \cos \bar{\omega} \bar{t})$ ,  $\epsilon \ll 1$ .

It should be noted that these authors have been interested in problems in which the amplitude of oscillation  $\epsilon$  is very small. However, there may be physical situations where  $\epsilon$  is not necessarily small. With this motivation, we have studied the fluctuating flow over a rotating disk with an angular velocity  $\Omega(1 + \epsilon \sin \bar{\omega} \bar{t})$ , where  $0 < \epsilon < 1$ . The problem cannot be handled by usual perturbation and asymptotic methods. The efficient finite difference is, therefore, used to analyze this problem with the effect of suction or injection. By using the von Kármán<sup>1</sup> type of similarity transformation, the governing equations are transformed to a set of partial differential equations in space variable  $\eta$  and time  $t$ . The question has been solved as an initial boundary-value problem, and the flow and heat-transfer characteristics have been studied for both short and long time ranges.

## Basic Equations

We choose cylindrical polar coordinates and assume the fluid to occupy the region  $z > 0$ , with the disk situated at the plane  $z = 0$ . Initially, the disk rotates with constant angular velocity  $\Omega$  about the axis  $r = 0$ , and there is a constant suction or injection  $h_0$  at the disk. At a particular instant of time, say,  $\bar{t} = 0$ , the angular velocity of the disk becomes  $\Omega(1 + \epsilon \sin \bar{\omega} \bar{t})$

due to superimposed torsional vibrations, where  $0 < \epsilon < 1$  is the amplitude and  $\bar{\omega}$  the frequency of oscillations. The fluid is assumed to be incompressible and to have constant physical properties. The conservation equations of mass, momentum, and energy in the absence of external body forces are

$$\frac{1}{r} \frac{\partial}{\partial r} (ur) + \frac{\partial w}{\partial z} = 0 \quad (1)$$

$$\frac{\partial u}{\partial \bar{t}} + u \frac{\partial u}{\partial r} + w \frac{\partial u}{\partial z} - \frac{v^2}{r} = -\frac{1}{\rho} \frac{\partial p}{\partial r} + \nu \left( \frac{\partial^2 u}{\partial r^2} + \frac{1}{r} \frac{\partial u}{\partial r} + \frac{\partial^2 u}{\partial z^2} - \frac{u}{r^2} \right) \quad (2)$$

$$\frac{\partial v}{\partial \bar{t}} + u \frac{\partial v}{\partial r} + w \frac{\partial v}{\partial z} + \frac{uv}{r} = \nu \left( \frac{\partial^2 v}{\partial r^2} + \frac{1}{r} \frac{\partial v}{\partial r} + \frac{\partial^2 v}{\partial z^2} - \frac{v}{r^2} \right) \quad (3)$$

$$\frac{\partial T}{\partial \bar{t}} + u \frac{\partial T}{\partial r} + w \frac{\partial T}{\partial z} = \frac{k}{\rho c_p} \left( \frac{\partial^2 T}{\partial r^2} + \frac{1}{r} \frac{\partial T}{\partial r} + \frac{\partial^2 T}{\partial z^2} \right) \quad (4)$$

where  $\rho$ ,  $\nu$ ,  $k$ , and  $c_p$  are the density, kinematic viscosity, thermal conductivity, and specific heat at constant pressure, respectively, and  $p$  is the pressure. The third momentum equation is useful in finding the pressure distribution only, and hence it is not considered in the present investigation.

The boundary conditions of the problem are

$$z = 0: \quad u = 0, \quad v = r\Omega(1 + \epsilon \sin \bar{\omega} \bar{t}), \quad w = h_0, \quad T = T_0 \quad (5)$$

$$z \rightarrow \infty: \quad u \rightarrow 0, \quad v \rightarrow 0, \quad T \rightarrow T_\infty \quad (6)$$

where  $T_0$  and  $T_\infty$  are, respectively, the temperatures of the disk and the ambient fluid.

The initial conditions are given by

$$u = u_i, \quad v = v_i, \quad w = w_i, \quad T = T_i \quad (7)$$

where  $u_i$ ,  $v_i$ ,  $w_i$ , and  $T_i$  represent the flow and temperature fields of the corresponding steady-state problem. It may be noted that the fluctuating flow problem is solved here as an initial boundary-value problem, starting with steady solutions of Eq. (7).

Using the transformations

$$\eta = (\Omega/\nu)^{1/2} z, \quad t = \Omega \bar{t}, \quad u = r\Omega F(\eta, t)$$

$$u = r\Omega(1 + \epsilon \sin \omega t) G(\eta, t)$$

$$w = (\nu\Omega)^{1/2} H(\eta, t), \quad p = \mu\Omega P(\eta, t)$$

$$(T - T_\infty)/(T_0 - T_\infty) = \Theta(\eta, t) \quad (8)$$

Received June 3, 1987; revision received April 21, 1988. Copyright © 1988 by K. A. Narayan. Published by the American Institute of Aeronautics and Astronautics, Inc., with permission.

\*Professor of Applied Mathematics.

†Graduate Student, Department of Mathematics.

‡Assistant Professor, Department of Chemical Engineering.

the governing equations, Eqs. (1-4), become

$$2F + \frac{\partial H}{\partial \eta} = 0 \quad (9)$$

$$\frac{\partial^2 F}{\partial \eta^2} - H \frac{\partial F}{\partial \eta} - F^2 + \varphi^2 G^2 - \frac{\partial F}{\partial t} = 0 \quad (10)$$

$$\frac{\partial^2 G}{\partial \eta^2} - H \frac{\partial G}{\partial \eta} - 2FG - \left( \frac{1}{\varphi} \frac{d\varphi}{dt} G + \frac{\partial G}{\partial t} \right) = 0 \quad (11)$$

$$\frac{1}{\sigma} \frac{\partial^2 \Theta}{\partial \eta^2} - H \frac{\partial \Theta}{\partial \eta} - \frac{\partial \Theta}{\partial t} = 0 \quad (12)$$

where  $\varphi(t) = 1 + \epsilon \sin \omega t$ ,  $\omega = \bar{\omega}/\Omega$  is the frequency parameter, and  $\sigma$  is the Prandtl number.

The transformed boundary conditions are

$$\begin{aligned} \eta = 0: \quad & F = 0, G = 1, H = H_0, \Theta = 1 \\ \eta \rightarrow \infty: \quad & F \rightarrow 0, G \rightarrow 0, \Theta \rightarrow 0 \end{aligned} \quad t \geq 0 \quad (13)$$

where  $H_0 = h_0/(\nu\Omega)^{1/2}$  is a suction parameter.  $H_0 > 0$  means injection, and  $H_0 < 0$  means suction. Equation (9), with the condition  $H = H_0$  at  $\eta = 0$ , can be written as

$$H = -2 \int_0^\eta F d\eta + H_0 \quad (14)$$

The initial conditions for the problem are obtained by solving the corresponding steady-state equations, which are obtained by putting

$$\varphi(t) = 1, \quad \frac{\partial F}{\partial t} = \frac{\partial G}{\partial t} = \frac{\partial \Theta}{\partial t} = 0$$

in Eqs. (10-12).

### Transformation to Finite Coordinates

The system of Eqs. (9-12) contains two independent variables  $\eta$  and  $t$ , varying from 0 to  $\infty$ . It is convenient from the computational point of view to transform these equations to a new system of coordinates wherein the indefinite limit of integration on  $\eta$  is replaced by a definite one. For this, we use the transformation

$$\xi = 1 - e^{-\alpha\eta} \quad (15)$$

suggested by Sills.<sup>9</sup> Here,  $\alpha$  is a constant that can be used as a scaling factor to provide an optimum distribution of nodal points across the boundary layer. In the present work,  $\alpha$  lies between 0.5 and 0.7, depending on suction parameter  $H_0$ . By using the transformation of Eq. (15), the interval  $\eta: [0, \infty]$  is transformed to  $\xi: [0, 1]$ . Denoting  $Z$  as  $Z = \alpha(1 - \xi)$ , we obtain the following set of equations for  $F$ ,  $G$ , and  $\Theta$ :

$$Z^2 \frac{\partial^2 F}{\partial \xi^2} - Z(H + \alpha) \frac{\partial F}{\partial \xi} - F^2 + \varphi^2 G^2 - \frac{\partial F}{\partial t} = 0 \quad (16)$$

$$Z^2 \frac{\partial^2 G}{\partial \xi^2} - Z(H + \alpha) \frac{\partial G}{\partial \xi} - 2FG - \left( \frac{1}{\varphi} \frac{d\varphi}{dt} G + \frac{\partial G}{\partial t} \right) = 0 \quad (17)$$

$$\frac{1}{\sigma} Z^2 \frac{\partial^2 \Theta}{\partial \xi^2} - Z \left( H + \frac{\alpha}{\sigma} \right) \frac{\partial \Theta}{\partial \xi} - \frac{\partial \Theta}{\partial t} = 0 \quad (18)$$

The initial conditions can be obtained now by putting

$$\varphi(t) = 1, \quad \frac{\partial F}{\partial t} = \frac{\partial G}{\partial t} = \frac{\partial \Theta}{\partial t} = 0$$

in Eqs. (16-18).

The boundary conditions now are

$$F = 0, G = 1, \Theta = 1 \text{ at } \xi = 0$$

$$F = G = \Theta = 0 \quad \text{at } \xi = 1 \quad t \geq 0 \quad (19)$$

In Eqs. (16-18),  $H$  is given by

$$H = 2 \int_0^\xi \left( \frac{F}{Z} \right) d\xi + H_0 \quad (20)$$

The solutions of the foregoing equations are useful in examining the velocity and temperature profiles at each instant of time  $t$ ; hence, the skin-friction and heat-transfer characteristics can be evaluated.

The nondimensional tangential skin friction is given by

$$S_1 = \frac{(\mu \partial v / \partial z)_{z=0}}{\rho r (\nu \Omega^3)^{1/2}} = \varphi \left( \frac{\partial G}{\partial \eta} \right)_{\eta=0} = \varphi \alpha \left( \frac{\partial G}{\partial \xi} \right)_{\xi=0} \quad (21)$$

and the radial skin friction in dimensionless form is

$$S_2 = \frac{\mu(\partial u / \partial z + \partial w / \partial r)_{z=0}}{\rho r (\nu \Omega^3)^{1/2}} = \left( \frac{\partial F}{\partial \eta} \right)_{\eta=0} = \alpha \left( \frac{\partial F}{\partial \xi} \right)_{\xi=0} \quad (22)$$

The surface heat-transfer rate is given by the Nusselt number as

$$Nu = \frac{-k(\partial T / \partial z)_{z=0}}{k(T_0 - T_\infty)} \left( \frac{\nu}{\Omega} \right)^{1/2} = - \left( \frac{\partial \Theta}{\partial \eta} \right)_{\eta=0} = - \alpha \left( \frac{\partial \Theta}{\partial \xi} \right)_{\xi=0} \quad (23)$$

By evaluating  $\partial G / \partial \xi$ ,  $\partial F / \partial \xi$ , and  $\partial \Theta / \partial \xi$  at  $\xi = 0$ , the variation of the skin frictions and surface rates of heat transfer to fluctuations in the angular velocity of disk can be studied.

### Numerical Solution and Results

The solutions of Eqs. (16-18), subject to the initial and boundary conditions, have been obtained by converting them into a set of implicit finite-difference equations of the Crank-Nicholson type. The resulting tridiagonal matrix equations are solved by the use of a suitable algorithm. The mesh point diagram for the Crank-Nicholson scheme is shown in Fig. 1. There are  $N$  nodal points in the  $\xi$  direction so that  $(N-1)\Delta\xi = 1$ , and the semisimilar equations (16-18) may be converted into a set of  $3(N-2)$  linear algebraic equations using the finite-difference formulations to approximate the unknowns and their derivatives. The tridiagonal equations can be written in a compact matrix form as

$$A_n \omega_{n-1} + B_n \omega_n + C_n \omega_{n+1} = D_n, \quad n = 2, 3, \dots, N-1 \quad (24)$$

with similar equations for  $G$  and  $\Theta$ .

The known matrices  $A_n$ ,  $B_n$ , and  $C_n$  and the vectors  $D_n$  are evaluated at  $(n, m)$  or  $(n, m + 1/2)$ , depending on the iteration. The system of Eqs. (24) will be complete by prescribing the values of the dependent variables at  $n = 1, N$ , which correspond to  $\xi = 0$  and  $\xi = 1$ , respectively, and are given by

$$\omega_1 = \begin{bmatrix} 0 \\ 1 \\ 1 \end{bmatrix}, \quad \omega_N = \begin{bmatrix} 0 \\ 0 \\ 0 \end{bmatrix} \quad (25)$$

Equations (24), together with the boundary conditions, [Eqs. (25)], form a set of linear algebraic equations and can be solved provided that the values of the dependent variables at the initial time  $t = 0$  are known.

We have used the following algorithm<sup>11</sup> to obtain the solution  $\omega_n$  at a certain instant  $t$ , i.e., for a particular value of  $m$ :

$$\omega_n = -E_n \omega_{n+1} + J_n, 1 \leq n \leq N-1 \quad (26)$$

where

$$E_n = (B_n - A_n E_{n-1})^{-1} C_n, 2 \leq n \leq N-1 \quad (27a)$$

$$J_n = (B_n - A_n E_{n-1})^{-1} (D_n - A_n J_{n-1}) \quad (27b)$$

and

$$E_1 = E_n = \begin{bmatrix} 0 & 0 & 0 \\ 0 & 0 & 0 \\ 0 & 0 & 0 \end{bmatrix}, J_1 = \begin{bmatrix} 0 \\ 1 \\ 1 \end{bmatrix}, J_n = \begin{bmatrix} 0 \\ 0 \\ 0 \end{bmatrix} \quad (28)$$

Knowing the values of the dependent variables and their derivatives at  $m$  corresponding to time  $t$ , the dependent variables  $\omega_n$  at  $m+1$ , which corresponds to time  $t + \Delta t$ , can be computed by adopting the following procedure. First, the values of the matrix elements  $A_{11}$ ,  $B_{11}$ , etc., are evaluated (see Appendix) using the known values of the variables  $F$ ,  $G$ , and  $\Theta$  at  $m$ . Next, with help of Eqs. (27) and (28), the  $E_n$  and  $J_n$  based on the values at  $m$  are calculated for all  $n$  between 1 and  $N$ , starting at the surface ( $n=1$ ) and proceeding toward the fluid at infinity ( $n=N$ ). The values of  $E_n$  and  $J_n$  are substi-

tuted in Eq. (26), and, by the use of the boundary conditions in Eq. (28),  $\omega_n$  at  $m+1$  are determined in reverse order, i.e., starting from  $n=N$ . New values of  $H$  at  $m+1$  are found from Eq. (20). The new values of  $H$  and  $\omega_n$  thus obtained are averaged over the interval with the corresponding values at  $m$  to form new matrix elements denoted by the indices  $(n, m + \frac{1}{2})$ , and the process of improving  $\omega_n$  at  $m+1$  is repeated until convergence is achieved. It is worthwhile to mention that the dependent variables with subscripts  $n$  and  $m$  need not be updated during the iteration process. The final values of  $\omega_n$  are again used to obtain  $\omega_n$  at  $m+2$ , and so on. At a particular instant of time  $t$ , the  $\xi$  derivatives at the surface are obtained by using a three-point derivative formula:

$$\left( \frac{\partial F}{\partial \xi} \right)_{\xi=0} = \frac{1}{2\Delta\xi} [-3F(0,t) + 4F(\Delta\xi,t) - F(2\Delta\xi,t)] \quad (29)$$

As the integral in Eq. (20) is singular at  $\xi=1$ , the value of  $H$  at  $\xi=1$  cannot be determined directly. So we have found the value of  $H$  at  $\xi=1$  by the extrapolation method.

The results were obtained for various values of the parameters  $\epsilon$ ,  $\omega$ , and  $H_0$  and a fixed Prandtl number  $\sigma = 0.7$ . To check the convergence of the finite-difference scheme, several values of step sizes  $\Delta\xi$  and  $\Delta t$  were used. Finally,  $\Delta\xi$  was taken to be 0.0125. As  $\omega$  increases, the value of  $\Delta t$  has to be decreased to get results of comparable accuracy. Actually,  $\Delta t$  is varied from 0.2 to 0.0025 when  $\omega$  is varied from 0.157 to 12.566. The comparison of skin-friction and surface heat-transfer results of the present study with those of Sparrow and Gregg<sup>10</sup> is shown in Table 1. The agreement is excellent in all cases.

In all of our computations, the solution for the unsteady case has been obtained for the first four cycles ( $\omega t = 8\pi$ ), and it is found that the transient effects die out within the first cycle in most cases. For comparing the results with available perturbation results, the computations were made for the case  $H_0 = 0$ ,  $\epsilon = 0.1$  (small amplitude), and  $\omega = 0.157$  and 12.566. The results are in good agreement, except for the difference in their phase angle by  $\pi/2$ . This is natural because we have taken the angular velocity of disk to be  $\Omega(1 + \epsilon \sin \bar{\omega} \bar{t})$ , whereas in Ref. 7 it is  $\Omega(1 + \epsilon \cos \bar{\omega} \bar{t})$ . For the case  $H_0 = 0$ , computations have been done for various values of  $\omega$  and  $\epsilon = 0.1, 0.3$ , and 0.5. The effects of amplitude  $\epsilon$  on the tangential and

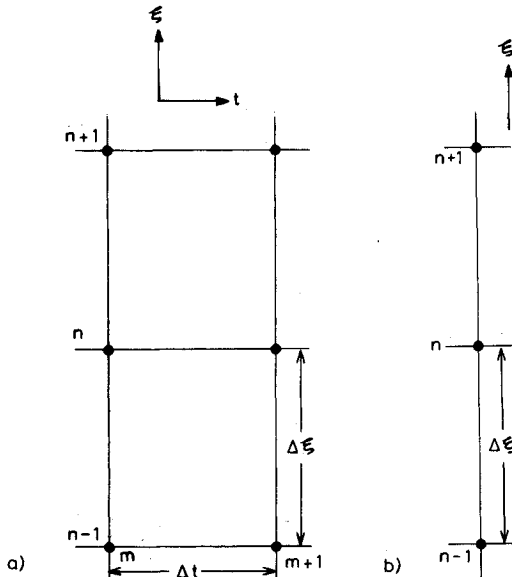


Fig. 1 Mesh point diagrams for Crank-Nicholson scheme: a) unsteady flow ( $t > 0$ ); and b) steady flow ( $t = 0$ ).

Table 1 Comparison of steady skin-friction and heat-transfer results with Sparrow and Gregg<sup>10</sup> for  $\sigma = 0.7$

| Present results |         |          |               | Ref. 3  |          |               |
|-----------------|---------|----------|---------------|---------|----------|---------------|
| $H_0$           | $F'(0)$ | $-G'(0)$ | $-\Theta'(0)$ | $F'(0)$ | $-G'(0)$ | $-\Theta'(0)$ |
| -1.5            | 0.3065  | 1.5801   | 1.0869        | 0.3068  | 1.580    | 1.087         |
| -0.8            | 0.4230  | 1.0365   | 0.6727        | 0.4232  | 1.036    | 0.6730        |
| 0               | 0.5103  | 0.6160   | 0.3231        | 0.5100  | 0.6159   | 0.3231        |
| 0.5             | 0.5147  | 0.4365   | 0.1782        | 0.5145  | 0.4364   | 0.1782        |
| 1.0             | 0.4896  | 0.3022   | 0.0854        | 0.4895  | 0.3022   | 0.0854        |

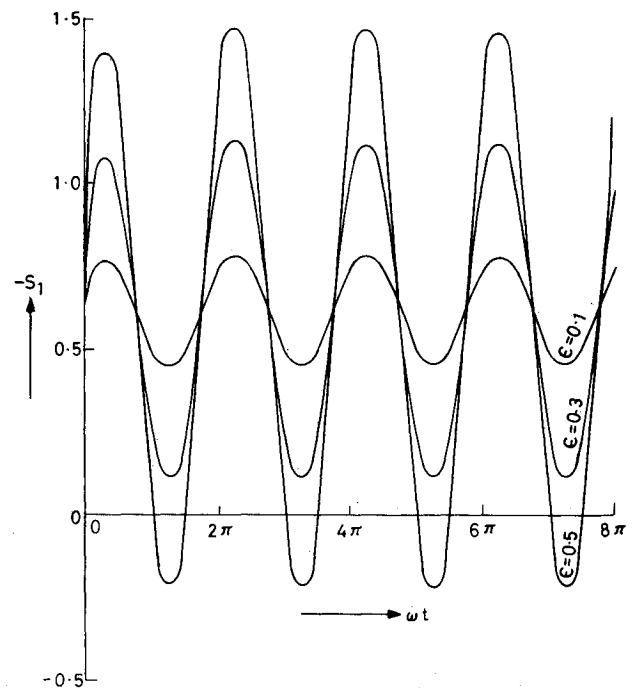


Fig. 2 Effect of amplitude on the tangential skin friction ( $H_0 = 0$ ,  $\sigma = 0.7$ ,  $\omega = 3.1416$ ).

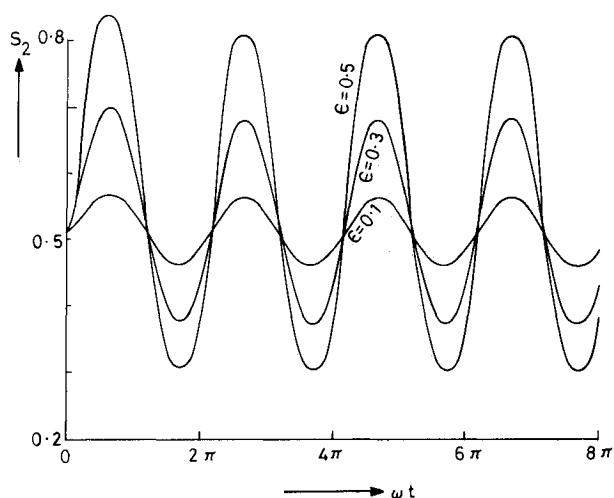


Fig. 3 Effect of amplitude on the radial skin friction ( $H_0 = 0$ ,  $\sigma = 0.7$ ,  $\omega = 3.1416$ ).

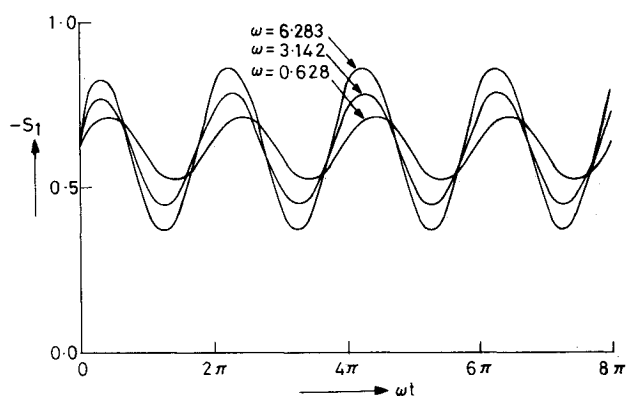


Fig. 4 Effect of frequency parameter on the tangential skin friction ( $H_0 = 0$ ,  $\sigma = 0.7$ ,  $\epsilon = 0.1$ ).

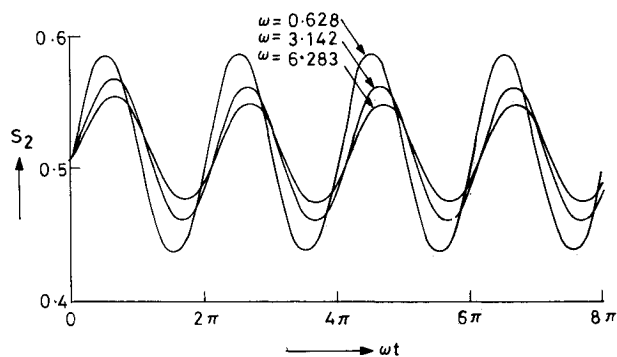


Fig. 5 Effect of frequency parameter on the radial skin friction ( $H_0 = 0$ ,  $\sigma = 0.7$ ,  $\epsilon = 0.1$ ).

radial skin friction are shown in Figs. 2 and 3. The amplitude of oscillations increases with  $\epsilon$ . For large values of  $\epsilon$  and  $\omega$ , the fluid adjacent to the disk rotates faster than the disk during part of each cycle. This can be inferred by a change in sign of  $S_1$ , as seen in Fig. 2 in the case  $\epsilon = 0.5$  and  $\omega = 3.1416$ .

The effects of frequency on the tangential and radial skin friction are shown, respectively, in Figs. 4 and 5. The amplitude of oscillations of the tangential skin friction increases and that of the radial skin friction decreases with  $\omega$ . The tangential skin friction is found to have a phase lead over the fluctuations of the disk's angular velocity, whereas the radial skin

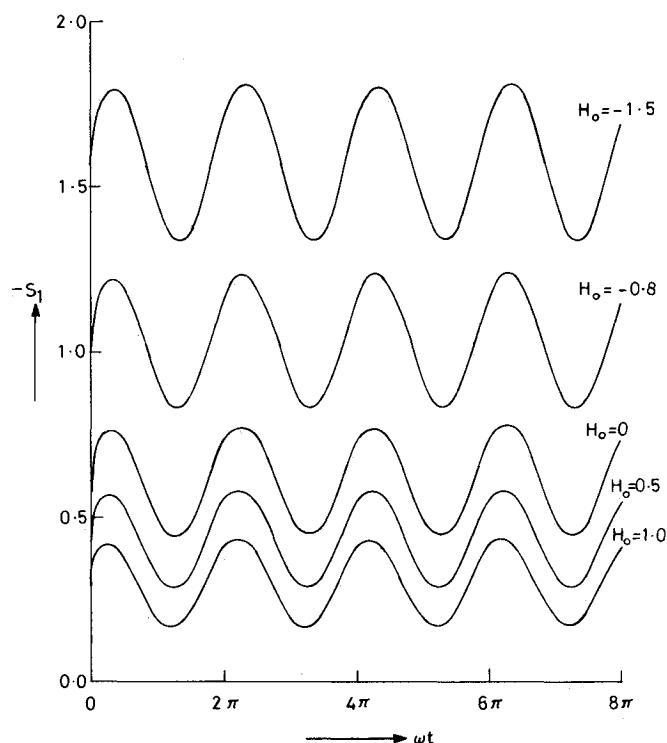


Fig. 6 Effect of suction and injection on the tangential skin friction ( $\sigma = 0.7$ ,  $\epsilon = 0.1$ ,  $\omega = 3.1416$ ).

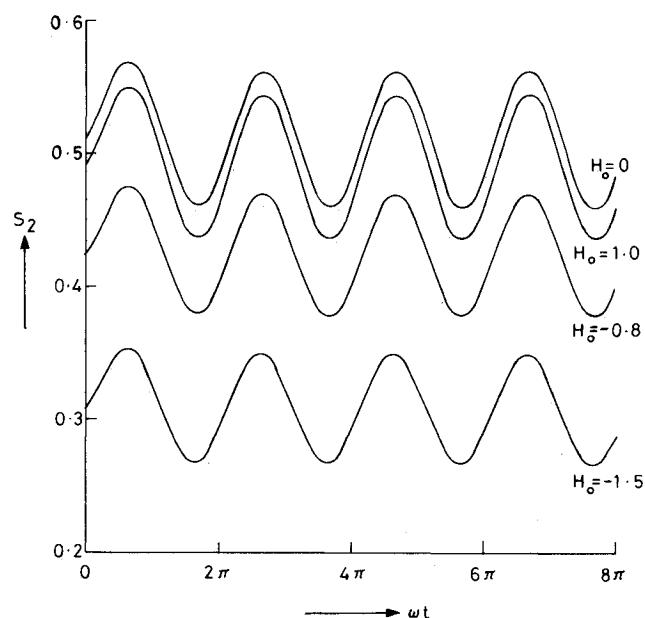


Fig. 7 Effect of suction and injection on the radial skin friction ( $\sigma = 0.7$ ,  $\epsilon = 0.1$ ,  $\omega = 3.1416$ ).

friction is found to have a phase lag. As  $\omega \rightarrow 0$ , the difference in the phase angle tends to zero. For large values of  $\omega$ , the phase lead of the tangential skin friction takes the value  $\pi/4$ , and the radial skin friction lags behind by  $\pi/4$ . These observations were found to be true even for large values of  $\epsilon$ . It is evident from Figs. 2-5 that the tangential skin friction responds more to the fluctuations in the disk angular velocity than the radial skin friction. The responses of surface heat transfer, as well as axial velocity at infinity, to fluctuations in the angular velocity of disk have also been studied. These fluctuations are very small and have not been represented in the figures. The phase angle of the surface heat transfer, as well as the axial velocity at infinity, lags behind that of the

disk's angular velocity, and their amplitudes decrease with  $\omega$ . For large values of  $\omega$ , the fluctuations in the surface heat transfer are negligible.

The suction and injection effects on the skin friction are shown in Figs. 6 and 7. Suction increases the tangential skin friction, whereas injection decreases it, as can be seen from Fig. 6. In the steady flow case, the radial skin friction attains a maximum value at around  $H_0 = 0.3$ , and this characteristic is maintained in the fluctuating case as well. The axial velocity at infinity responds more to the fluctuations in the disk's angular velocity in the case of injection than to the suction.

### Appendix

The matrix elements in Eq. (24) are given by

$$A_{11} = A_{22} = \frac{Z^2}{2(\Delta\xi)^2} + \frac{Z}{4\Delta\xi} (H + \alpha) \quad (A1)$$

$$A_{33} = \frac{Z^2}{2\sigma(\Delta\xi)^2} + \frac{Z}{4\Delta\xi} \left( H + \frac{\alpha}{\sigma} \right) \quad (A2)$$

$$C_{11} = C_{22} = -A_{11} + \frac{Z^2}{(\Delta\xi)^2} \quad (A3)$$

$$C_{33} = -A_{33} + \frac{Z^2}{\sigma(\Delta\xi)^2} \quad (A4)$$

$$B_{11} = -\frac{Z^2}{(\Delta\xi)^2} - F_{n,m} - \frac{1}{\Delta t} \quad (A5)$$

$$B_{12} = \varphi^2 G_{n,m} \quad (A6)$$

$$B_{21} = -G_{n,m} \quad (A7)$$

$$B_{22} = B_{11} - \frac{1}{2\varphi} \frac{d\varphi}{dt} \quad (A8)$$

$$B_{33} = -\frac{Z^2}{\sigma(\Delta\xi)^2} - \frac{1}{\Delta t} \quad (A9)$$

$$D_1 = \frac{-Z^2}{2} \frac{\partial^2 F_{n,m}}{\partial \xi^2} + \frac{Z}{2} (H + \alpha) \frac{\partial G_{n,m}}{\partial \xi} - \frac{F_{n,m}}{\Delta t} \quad (A10)$$

$$D_2 = \frac{-Z^2}{2} \frac{\partial^2 G_{n,m}}{\partial \xi^2} + \frac{Z}{2} (H + \alpha) \frac{\partial G_{n,m}}{\partial \xi} - \frac{G_{n,m}}{\Delta t} + \frac{1}{2\varphi} \frac{d\varphi}{dt} G_{n,m} \quad (A11)$$

$$D_3 = -\frac{Z^2}{2\sigma} \frac{\partial^2 \Theta_{n,m}}{\partial \xi^2} + \frac{Z}{2} \left( H + \frac{\alpha}{\sigma} \right) \frac{\partial \Theta_{n,m}}{\partial \xi} \quad (A12)$$

where

$$\frac{\partial F_{n,m}}{\partial \xi} = \frac{1}{2\Delta\xi} (F_{n+1,m} - F_{n-1,m}) \quad (A13)$$

$$\frac{\partial^2 F_{n,m}}{\partial \xi^2} = \frac{1}{\Delta\xi^2} (F_{n+1,m} - 2F_{n,m} + F_{n-1,m}) \quad (A14)$$

with similar expressions for  $G$  and  $\Theta$ .

### References

- <sup>1</sup>von Kármán, T., "Über Laminare und Turbulente Reibung," *ZAMM* Vol. 1, Jan. 1921, pp. 244-247.
- <sup>2</sup>Rosenblatt, S., "Torsional Oscillations of a Plane in a Viscous Fluid," *Journal of Fluid Mechanics*, Vol. 6, Aug. 1959, pp. 206-220.
- <sup>3</sup>Benney, D. J., "The Flow Induced by a Disk Oscillating in its Own Plane," *Journal of Fluid Mechanics*, Vol. 18, March 1964, pp. 385-391.
- <sup>4</sup>Schippers, H., "Analytical and Numerical Results for the Non-Stationary Rotating Disk Flow," *Journal of Engineering Mathematics*, Vol. 13, April 1979, pp. 173-191.
- <sup>5</sup>Riley, M., "Oscillating Viscous Flows," *Mathematika*, Vol. 12, June 1965, pp. 161-175.
- <sup>6</sup>Lighthill, M. J., "The Response of Laminar Skin Friction and Heat Transfer to Fluctuations in the Stream Velocity," *Proceedings of the Royal Society of London*, Vol. A224, June 1954, pp. 1-23.
- <sup>7</sup>Purushothaman, R., "Fluctuating Flow Due to a Rotating Disk," *Physics of Fluids*, Vol. 21, No. 3, Dec. 1978, pp. 2148-2153.
- <sup>8</sup>Sharma, V. P., "Flow and Heat Transfer Due to Small Torsional Oscillations of a Disk About a Constant Mean," *Acta Mechanica*, Vol. 32 (1-3), April-July 1979, pp. 19-34.
- <sup>9</sup>Sills, J. A., "Transformations for Infinite Regions and their Application to Flow Problems," *AIAA Journal*, Vol. 7, Jan. 1969, pp. 117-123.
- <sup>10</sup>Sparrow, E. M. and Gregg, J. L., "Mass Transfer Flow, and Heat Transfer About a Rotating Disk," *Journal of Heat Transfer*, Vol. 82, June 1960, pp. 294-302.
- <sup>11</sup>Varga, R. S., *Matrix Iterative Analysis*, Prentice-Hall, Englewood Cliffs, NJ, 1962, p. 194.